Hydrothermal crystallization of clathrasils in acidic medium: energetic aspects

Haonuan Zhao, Qiaolin Lang, Guangying Fu, Ruiqin Ding, Songxia Wang, Xiaobo Yang, Valentin Valtchev

Hydrothermal crystallization of clathrasils in acidic medium: energetic aspects

Haonuan Zhao,[a,b] Qiaolin Lang,[a] Guangying Fu,[a] Ruiqin Ding,[a] Songxia Wang,[a] Xiaobo Yang,[*,a] Valentin Valtchev[**,a,b]

[a] The ZeoMat Group, Qingdao Institute of Bioenergy and Bioprocess Technology, CAS, Laoshan District, CN-266101 Qingdao, China.

[b] Normandie University, ENSICAEN, UNICAEN, CNRS, Laboratoire Catalyse et Spectrochimie, F-14000 Caen, France.

E-mail: yangxb@qibebt.ac.cn, valentin.valtchev@ensicaen.fr

ABSTRACT

A series of clathrasils, including **AST**, **DOH**, **MTN,** and **DDR** topologies, were synthesized in an acidic medium. The general composition of the initial system was 1 SiO_2: 0.3-0.5 SDA: 0.1-0.5 HF/NH_4F: 0-0.3 HBr: 10-50 H_2O in the pH range of 2-6, where SDA stands for organic amines or ammonium ions as the structure-directing agents. And the hydrothermal syntheses were performed in the 150-200°C temperature range. Besides elaborating the synthesis recipes and product characterizations, the study also attempted to elucidate the origins of slow crystallization kinetics. It was found that the thermodynamic stabilities of the SDA@Framewrok-SiO_2 compounds play an overwhelming role in the crystalline phase selection. The finding of this study can be used as a guidance of silica-based porous materials synthesis under acidic conditions.

Keywords: clathrasil, zeolite, synthesis, acidic medium

1. INTRODUCTION

Clathrasils, or clathrate compounds of silica, are inclusion compounds with molecular guest species encapsulated in crystalline silica frameworks. The frameworks are composited of SiO_4-tetrahedra building up cage-type structures in a way similar to the 4-connected frameworks of H_2O molecules linked via H-bonds in clathrate hydrates [1, 2]. The cage-like void spaces of clathrasil structures, where the guest species reside, possess sub-nanometer dimensions (tens to hundreds cubic Angstroms in volume). And the cages are accessible

through rings of not greater than 6-members of SiO_4-tetrahedra. This feature distinguishes the clathrasils from pure-silica zeolites with the respect that zeolites' open-framework structures, which are as well made of corner-sharing SiO_4-tetrahedra, have windows of sizes bigger than 6-membered rings accessing the intracrystalline cages or channels [3, 4]. The small openings of clathrasils' cages allow only the smallest molecules, i.e., He and H_2, to diffuse through them. For example, clathrasils may be applied as membranes or fillers in polymeric composite membranes for CO_2/H_2 separation [5-8].

The clathrasil minerals found in Nature so far, i.e., melanophlogite (framework topology code **MEP**) [2], Holdstite (**MTN**) [9], chibaite (**MTN**) [10], and bosoite (**DOH**) [11], occlude as guest molecules N_2, CO_2, light hydrocarbons like CH_4, C_2H_6, and sometimes noble gases or other impurities.

Different from the minerals, synthetic clathrasils contain in their void spaces structure-directing agents (SDA). The method to synthesize clathrasils is analog to that for the syntheses of pure-silica zeolites, where hydrothermal crystallization is performed in silica hydrogels containing organic ammonium ions or amine molecules as the SDA.

ZSM-39 (**MTN**) was the first synthetic clathrasil, which was synthesized using tetramethylammonium and tetraethylammonium ions as SDA [1]. The dodecasil series synthesized by Liebau, Gies, and Gerke crystallize with various amines as SDA under the protection of inert gases [12]. Specifically, dodecasil 1H (**DOH**) crystallizes at the presence of piperidine and N_2 [13], or 1-aminoadamantane and N_2 [14]; dodecasil 3C (**MTN**) forms at the presence of trimethylamine in a gas mixture out of N_2, Ar, Kr, CH_4 or CO_2 [12, 15].

Related to dodecasils, deca-dodecasil 3R (**DDR**) crystallizes in the presence of 1-aminoadamantane and ethylenediamine. Like the dodecasils, **DDR** structure possesses the same pentagonal dodecahedron [5^{12}] as a building unit. However, through a different stacking of the dodecahedron layers, another small decahedron cage [$4^3 5^6 6^1$] and a bigger 19-hedraon cage [$4^3 5^{12} 6^1 8^3$] arise in **DDR**. The big cage has 8-ring windows forming 2-dimmentional passages. **DDR** possesses both closed and open cages, and stands as a link between zeolites and clathrasils [16].

Nonasil (**NON**) can be synthesized using a number of amines as SDA, including 2-methyl-pyrrolidine, hexamethylene-imine, 2-aminomethyl-tetrahydrofuran, 1,2-diamino-cyclohexane, 2-methyl-piperidine, 2-methyl-piperazine, 1-amino-butane, 2-amino-butane, and 2-amino-pentane, in Ar atmosphere [17]. Recently, using Gemini-type surfactants as SDA a nonasil-related material (ECNU-27) has been synthesized, which possesses defective 8-ring channels due to the lang chains of the SDA, enabling the material to be used as a catalyst [18].

Another clathrasil synthesized with 1-aminoadamantane as the SDA is Sigma-2 (**SGT**) [19, 20]. Sigma-2 can also crystallize at the presence of 3-azabicyclo[3.2.2]nonane as SDA [21].

RUB-10 (**RUT**) is a clathrasil with tetramethyl-ammonium as the SDA. In its structure, there is a big cage with an 8-ring window. However, every two adjacent cages share the window, thereby closing the pathways of each other [22].

The hydrothermal syntheses of the above materials are carried out with basic hydrogels at 150-200^{o}C in several days to several months.

Fluoride media of near-neutral pH have been applied for the crystallization of clathrasils, as well. Octadecasil (**AST**) was synthesized by Caullet et al. in fluoride media at pH 6-9 using tetramethyl-ammonium (TMA^+) or quinuclidinium (Q^+) cations as SDA [23]. Pang et al. also attempted to synthesize other clathrasils in near-neutral fluoride media with respective SDAs, where the crystallization of ZSM-39 and nonasil was successful [24].

Recently, Valtchev et al. have demonstrated that high-silica and pure-silica zeolites can crystallize in strongly acidic fluoride media [25, 26]. Essentially, the system pH should stay above the isoelectric point of the dissolved silicate species, which is around ca. 2.3 depending on the silica source, concentrations, and other conditional parameters, in order to establish proper interactions between SDA and the silicate species while the crystallization proceeds. This discovery greatly expands the chemical field of zeolite crystallization. Furthermore, it enables the use of those SDA and chemical elements in the zeolite syntheses that otherwise decompose or precipitate at higher pH, opening ways to new structures and new framework compositions.

The present paper illustrates that the method to synthesize zeolites in strongly acidic fluoride media can be adapted to the syntheses of several clathrasils. Since tetrametylammonium ions, and 1-aminoadamantane are often used SDAs in the syntheses of clathrasils and zeolites, together with hexamethylenetetramine (HMTA), which has a similar shape of adamantane, they are selected as the experimental objects. Some general aspects encountered during the slow nucleation and crystal growth processes and some experimental parameters affecting the phase selection and crystal morphologies are elaborated. The experimental results show, that the crystallization in an acidic medium is a generally applicable method for the synthesis of many framework silicate materials; and HMTA is the first SDA example that does not work in the traditional basic and neutral systems but leads to a successful crystallization of deca-dodecasil 3C under the acidic condition.

2. EXPERIMENTAL

2.1 Hydrothermal synthesis

Materials. Tetramethylammonium hydroxide (TMAOH, 25 wt.% aq., Aladine), 1-aminoadamantane (ADA, >98%, Macklin), hexamethylenetetramine (HMTA, P.A. Sinopharm), hydrobromic acid (HBr, 40 wt.% aq., Aladine), hydrofluoric acid (HF, 40 wt.% aq., Macklin), LUDOX AS-40 colloidal silica (40 wt.% suspension in H_2O, Aldrich), and deionized (DI) water were used in the synthetic experiments. All reagents were used as received without further purification.

Synthesis. Clathrasils were synthesized with different structure-directing agents (SDA), using gels with molar compositions 1.0 SiO_2: 0.5 SDA: x (NH_4F/HF): y HBr: z H_2O. The successful syntheses are presented in Table 1. Respective SDA was first dissolved in water, followed by the addition of a silica source. This mixture was stirred for 18 hours at room temperature. Then NH_4F/HF/HBr solutions were added to the gel and stirred for another 5-10 min. The homogenized reaction mixtures were sealed in Teflon-lined stainless-steel autoclaves. The crystallizations were performed statically at 150 - 200°C for several days. The recovered solid products were washed three times with water and dried at 80°C in air. A portion of the starting

gels was centrifuged at 30.000 rpm for 1 hour. The pH values of the supernatant liquids were recorded.

Table 1. The synthetic recipes, hydrothermal parameters, and corresponding products.

Exp#	SDA	Gel composition (molar ratio)	pH	T(°C)	t(days)	Product
AST-1	TMA^+	$1SiO_2$:0.5TMAOH:0.5HF:$4H_2O$	8.1	180	10	**AST**
AST-2	TMA^+	$1SiO_2$:0.2TMAOH:0.3TMABr:0.5HF:$10H_2O$	4.2	150	10	**AST**
DOH-1	ADA	$1SiO_2$:0.5ADA:0.5HF:$60H_2O$	8.4	200	10	**DOH**
DOH-2	ADA	$1SiO_2$:0.5ADA:0.5HF:0.2HBr:$60H_2O$	1.5	200	10	**DOH**
MTN-1	HMTA	$1SiO_2$:0.5HMTA:0.056NH_4F:0.083HF:$50H_2O$	6.1	160	21	**MTN**
MTN-2	HMTA	$1SiO_2$:0.5HMTA:0.125HF:0.1HBr:$20H_2O$	4.4	160	39	**MTN**
DDR-1	ADA	$1SiO_2$:0.5ADA:0.5HF:$20H_2O$	6.2	160	14	**DDR**
DDR-2	ADA	$1SiO_2$:0.5ADA:0.5HF:0.2HBr:$20H_2O$	1.6	180	10	**DDR**

2.2 Characterization

Crystalline products were identified by powder X-ray diffraction at room temperature in ambient air on a RIGAKU SmartLab Diffractometer. The diffractometer uses Cu Kα radiation (λ = 1.5418 Å, 40 kV, 150 mA) with a scanning speed of 20.00°/min at 0.01° steps in the theta-theta geometry. Samples were pressed on a glass plate.

Scanning Electron Microscopy (SEM) of the samples were recorded on JEOL JSM-6700F Microscope, which was equipped with a cold field emission gun operated at 1~2 kV.

^{29}Si MAS NMR experiments were performed on Bruker AVANCE III 600 spectrometer at a resonance frequency of 119.2 MHz. ^{29}Si MAS NMR spectra with high-power proton decoupling were recorded on a 4 mm probe with a spinning rate of 10 kHz, a π/4 pulse length of 2.6 μs, and a recycle delay of 60 s. The chemical shifts of ^{29}Si are referred to TMS.

TG/DTA analysis was performed using Rigaku TG-DTA8122 microbalance upon ca. 10 mg zeolite powder against α-Al_2O_3, in 50 ml/min reconstituted (80% N_2 + 20% O_2) airflow at a heating rate of 10°C/min in the temperature range from room temperature to 1300°C.

2.3 Molecular simulations

The amount of a particular SDA occluded in a clathrasil or zeolite framework at 298 K and 101.3 kPa was simulated using the Sorption module of Materials Studio. A framework cut of ca. 20-30 Å in edges (2 X 2 X 2 unit cells for **AST** and **DOH**, 1 X 1 X 1 for **MTN**, and 2 X 2 X 1 for **DDR**) and P1 symmetry was put into the pcff force field, where locations and configurations of SDA were tested in energy minimization. 5 X 10^6 configurations of the SDA were generated by the Monte Carlo method Metropolis [27]. The isosteric heat was taken as a measure of the net gain of energy upon forming the SDA@Framework compound. The

location of SDA was then confirmed using Sorption Locate, and again, by Adsorption Locator, both are simulated annealing protocols with geometric optimizations but with different cooling algorisms [28]. The Adsorption Locator led to more relaxations, thus higher isosteric heats. For comparison, tetra-n-propylammonium ion (TPA^+) in the **MFI** framework was taken to perform the same simulation procedure as a ball par.

Table 2 lists the structure cuts of the frameworks that were subjected to the simulation. The unit cell parameters of **DOH**, **MTN** and **DDR** were taken from the Material Studio structure database. The unit cell of [SiO_2]-**AST** framework was taken from the structure database of the International Zeolite Association [29].

Table 2: The unit cell parameters and the framework cut used in the simulations.

Framework	SDA	Unit cell	Simulation cut
AST	TMA^+	Fm3m (#225) a = 13.624 Å	27.248*27.248*27.248 $Å^3$
DOH	ADA	P6/mmm (#191) a = 13.782976, c = 11.190 Å, γ = 120°	27.565952*27.565952*22.380 $Å^3$
MTN	HMTA	Fd3m (#227) a = 19.402 Å	19.402*19.402*19.402 $Å^3$
DDR	ADA	R-3m (#166) a = 13.85999, c = 40.892 Å, γ = 120°	27.71998*27.71998*40.892 $Å^3$
MFI	TPA^+	Pnma (#62) a = 20.022, b = 19.899, c=13.383 Å	20.022*19.899*26.766 $Å^3$

3. RESULTS AND DISCUSSIONS

3.1 The successful syntheses of clathrasils in acidic medium

The syntheses of the clathrasils, including TMA^+/**AST**, ADA/**DOH**, HMTA/**MTN** and ADA/**DDR**, were successful at the presence of fluoride ions in silica hydrogels of various pH values, at the conditions illustrated in Table 1. Their XRD patterns are shown in Figure 1, SEM pictures in Figure 2. The crystals obtained at different pH exhibit different sizes and habits, which are observed by SEM, and by powder XRD in the diffractograms as preferred orientations to particular crystallographic planes.

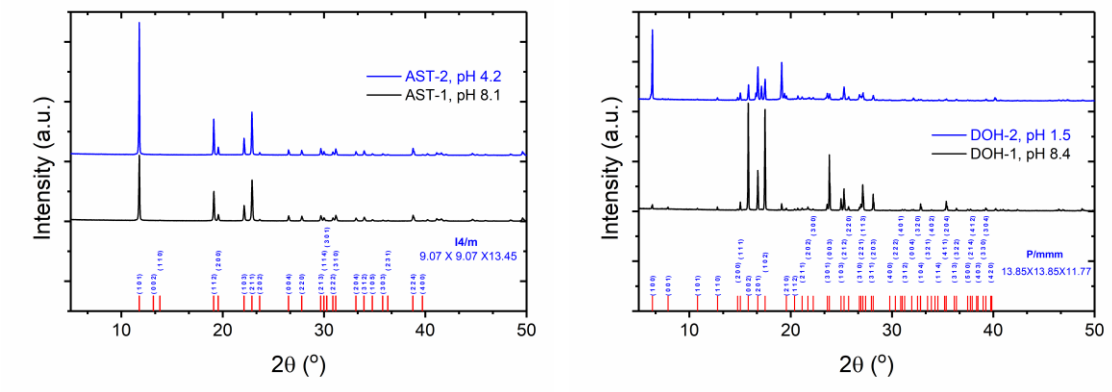

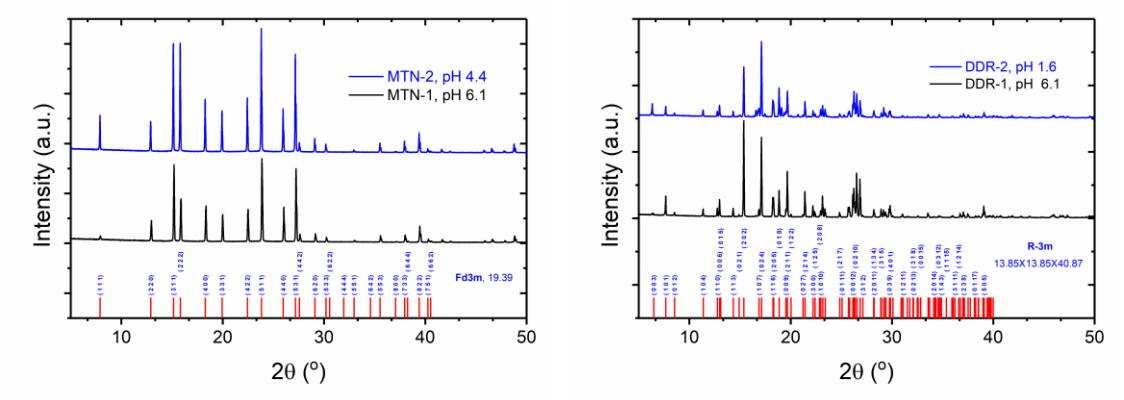

Figure 1. XRD patterns of the clathrasils crystallized from hydrogels of various pH values (Sample numbers according Table 1). The red droplines indicate reflection positions of respective (hkl) planes indexed in the unit cells with symmetries and parameters as the notations.

Adapted from the method of Caullet et al. [23], a gel has been prepared with the composition 1 SiO_2: 0.5 TMAOH: 0.5 HF: 4 H_2O, using freeze-dried Ludox AS40 as the silica source. When centrifuged at 30000 rpm for 60 min, the liquid supernatant has a pH = 8.1. The gel crystallizes at 180°C in 10 days into |TMA^+, F^-|-[SiO_2]-octadecasil-**AST** [30]. Replacing a portion of TMAOH with TMABr, the gel of the composition 1 SiO_2: 0.2 TMAOH: 0.3 TMABr: 0.5 HF: 4 H_2O at pH = 4.2 has been obtained. |TMA^+, F^-|-[SiO_2]-octadecasil-**AST** crystalizes from this gel at 150°C in 10 days. Both octadecasil materials show the same XRD patterns, which are in accordance with **AST** framework topology (Figure 1). In these materials, TMA^+ cation is occluded in the rhombo-octadecahedral [$4^6 6^{12}$] cage, F^- anion in the hexahedral [4^6] cage [30]. The calcination procedure has been extensively studied, to remove the occluded species and make the cages free for adsorptive applications [31]. SEM pictures (Figure 2) show that the product of basic medium synthesis is highly agglomerated as the individual crystallites range from submicron to a few micrometers in size. The acidic medium crystals are bigger, in the range of 20-40 μm, with well-developed crystal surfaces and less intergrown. In XRD, both materials can be indexed in a unit cell of the tetragonal space group I4/m (#87) [30, 31], with the unit cell parameters a = b = 9.07 Å, c = 13.45 Å, α, β, γ = 90°. The low-pH product's (101) peak has an observably exaggerated intensity because the large crystals with well-developed surfaces lie preferentially on this plane on the plate sample holder in the theta-theta measurement.

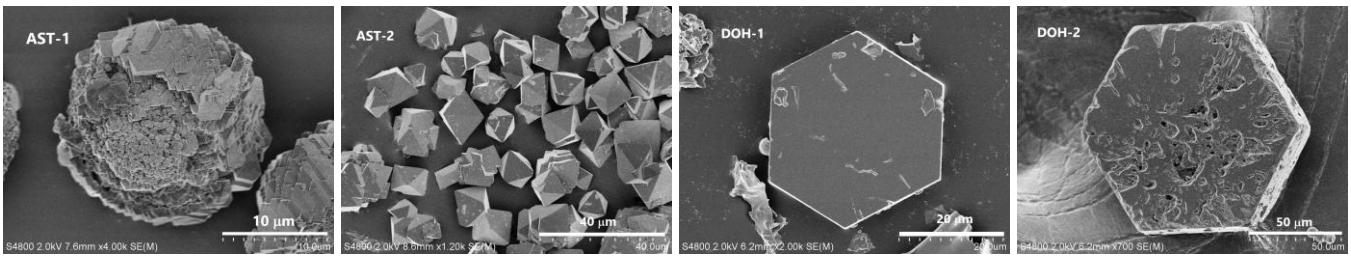

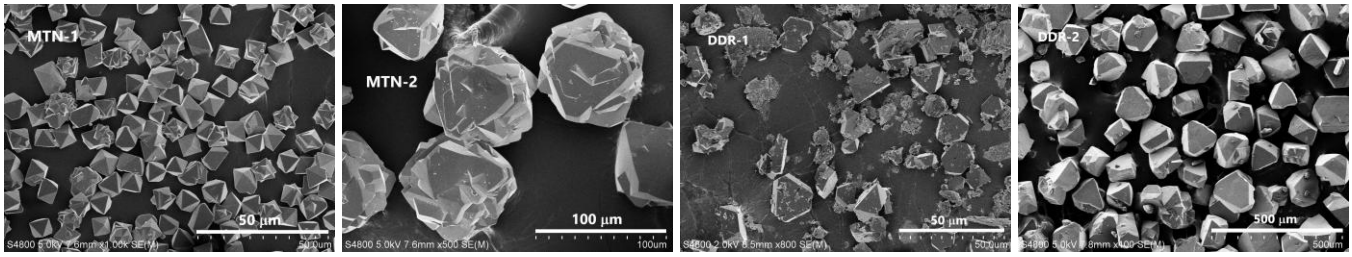

Figure 2. SEM pictures of the clathrasils crystallized from hydrogels of various pH values (Sample numbers according Table 1).

Dodecasil 1H-**DOH** was first synthesized by Gerke and Gies using piperidine as SDA at 250^{o}C [13]. Latter, Gies disclosed another recipe to crystallize the same framework in the presence of 1-aminoadamantane (ADA) at 200^{o}C [14].

We prepared a gel of the composition 1 SiO_2: 0.5 ADA: 0.5 HF: 60 H_2O, which has a pH of 8.4. It crystallizes into dodecasil 1H-DOH at 200^{o}C in 10 days. Then we pushed the pH of the gel to 1.5 by adding 0.2 molar equivalent HBr (relative to SiO_2). The gel 1 SiO_2: 0.5 ADA: 0.5 HF: 0.2 HBr: 60 H_2O crystallizes to dodecasil 1H-**DOH** at 200^{o}C in 10 days, too. The XRD and SEM analyses of the product are shown in Figure 1 and Figure 2, respectively. The significant differences in the relative diffraction intensities of diverse crystallographic planes among the two samples imply preferred orientations. SEM (Figure 2) confirms this observation. In both cases, dodecasil 1H crystals exhibit the hexagonal plate shape. But they are different in sizes and aspect ratios. The plate diameter of the basic medium product is averaged at 20 μm, while the one of the acidic medium product is 110 μm. Traces of dissolution of the pinacoidal face can be observed in the crystals obtained in an acidic medium, which is most probably due to the too long crystallization time. Both materials can be described with the hexagonal P/mmm (#191) unit cell of a = b = 13.85 Å, c = 11.77 Å, α, β = 90^{o}, γ = 120^{o}. Compared to the acidic product, the sample synthesized at higher pH has a very big aspect ratio along the directions of a, b versus c. Therefore, its XRD shows a preferred orientation along the c axis, i.e., the peaks (001), (002), (003) are abnormally profound.

Dodecasil 3C-**MTN** [12], or ZSM-39 [1], can be synthesized in basic medium using tetramethyl-ammonium, 1-aminoadamantane, and a number of other organic amines as SDA [14, 32, 33]. With TMA^{+} as SDA, it crystallizes in a near-neutral fluoride medium as well [24].

Hexamethylenetetramine (HMTA) molecule has the same shape as adamantane, but with four N atoms at the vertexes of cycles instead of C atoms. A vast number of amines and organic ammonium ions of similar cyclic and polycyclic shapes were tested as SDAs in the synthesis of clathrasils and zeolites [34-37]. However, HMTA has been overlooked so far, probably due to the low C/N ratio of 1.5, which is far below the thumb-rule range of 10-16 for SDA candidates that offer balanced hydrophobicity/hydrophilicity during the framework crystallization, as proposed by Zones et al. [38-40]. It means, that HMTA in aqueous phase has a strong hydrate shield that is hardly exchangeable with the solute silicate species. Therefore, it is not a powerful SDA in crystallizing porous framework silicates.

However, we now have observed that in the acidic medium of the pH range between 4-6

HMTA works as a selective and robust SDA for dodecasil 3C in a broad range of water dilution (H_2O/SiO_2 = 20-50). XRD patterns of two highly crystalline products obtained at various conditions are shown in Figure 1. The gel 1 SiO_2: 0.5 HMTA: 0.056 NH_4F: 0.083 HF: 50 H_2O has a pH of 6.1, and crystallizes at 160°C in 21 days. 1 SiO_2: 0.5 HMTA: 0.125 HF: 0.1HBr: 20 H_2O has a pH of 4.4, and it takes 39 days for dodecasil 3C-**MTN** to crystallize from this low pH gel at 160°C. SEM pictures of both products are seen in Figure 2. The product obtained at pH = 6.1 are octahedral crystals and rarely intergrown particles, with ca. 10 μm edge lengths. The pH = 4.4 synthesis yields much bigger intergrown octahedral crystals of ca. 80 μm in edge length. The XRD peaks can be indexed in the cubic Fd3m (#227) unit cell of a = 19.39 Å. The (111) face is the most exposed face of these crystals; therefore, the bigger crystals prefer to lie on it and accentuate the intensity of (111), (222) peaks.

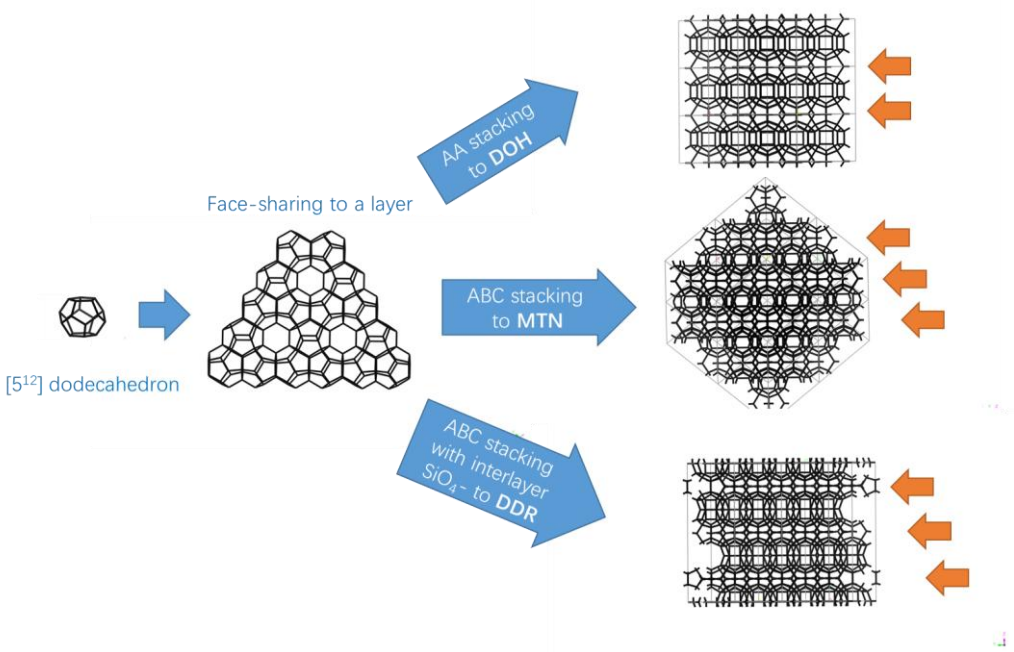

Chart 1. Face-sharing [5^{12}] dodecahedra built a layer. The layer stacking in different sequences forms **DOH**, **MTN,** and **DDR** frameworks, respectively.

As described by Gies, deca-dodecasil 3R-**DDR** is the link between zeolites and clathrasils, in the sense that its framework is constructed with the same building units as the dodecasil series. The common building unit is a pentagonal dodecahedron [5^{12}] cage, which links into a pseudohexagonal layer by sharing the pentagonal faces. As shown in Chart 1, stacking the identical layers in different sequences results in the frameworks of dodecasil 1H-**DOH** (AA stacking in hexagonal symmetry), dodecasil 3C-**MTN** (ABC stacking in cubic symmetry), and deca-dodecasil 3R **DDR** (ABC stacking with interlayer SiO_4-units in rhombohedral symmetry) [12, 15, 16].

Deca-dodecasil 3R was synthesized using 1-aminoadamantane (ADA) as the SDA at 170°C for a relatively long time, up to 10 weeks [16]. Its isostructural variant ZSM-58 was synthesized using methyltropinium ion as the SDA at 160°C in a few days [41-43]. We used 1-aminoadamantane as the SDA, and prepared a gel with composition 1SiO_2: 0.5 ADA: 0.5

HF: 20 H_2O, which had a pH of 6.2. It crystallizes to deca-dodecasil 3R-**DDR** at 180^{o}C in 10 days (Figure 1). The crystals have irregularly truncated octahedral shapes of 20 μm in edges, but with quite number of amorphous impurities (Figure 2). In a very acidic medium at pH = 1.6 using a gel of the composition 1SiO_2: 0.5 ADA: 0.5 HF: 0.2 HBr: 20 H_2O, deca-dodecasil 3R-**DDR** crystalized at 180^{o}C in 14 days into big and clean crystals, also of truncated octahedral shapes. The edge lengths are around 100 μm (Figure 2). The XRD patterns in Figure 1 show a rhombohedral R-3m (#166) cell of a, b = 13.85 Å and c = 40.87 Å, α, β = 90^o, γ = 120^o. The preferred orientation is (101), thus, the peaks of (101), (202) are more intense for the thinner crystals obtained at higher pH.

3.2 Framework integrity and imperfection of the materials obtained in acidic media

A common feature in the synthesis of SDA@SiO_2 compounds in the acidic fluoride medium is the big crystal sizes as a consequence of the low nucleation rate and slow growth (>10 days), which is substantially longer compared the syntheses of most zeolites at basic conditions. It is known that the zeolites obtained via the fluoride route usually contain less-point defects, thus possess a framework with better local orders and higher integrity [35, 44]. And this effect becomes more profound in the acidic medium [25, 26]

^{29}Si MAS NMR in Figure 3 in principle supports that this trend holds with the acidic medium synthesized clathrasils, by showing well-resolved peaks that can be attributed to different crystallographic T sites. However, materials with local structural imperfections may occur in an acidic medium as well, probably due to the not optimized recipes of individual synthetic batches.

The ^{29}Si MAS NMR of |TMA^+,F^-|[SiO_2]-octadecasil-**AST** sample synthesized at pH = 4.2 (Sample AST-2) shows two well-resolved sharp Q4 (Si-(O-Si)$_4$) peaks at δ = -106.15 and -107.47 ppm, with an area ratio of 4:1. In the tetragonal I4/m (#87) unit cell, |TMA^+,F^-|[SiO_2]-octadecasil-**AST** compound has two unique framework T positions: Si1 on the general position of (0.2328, 0.0453, 0.11274) and Si2 on the special position (0, 0.5, 0.25). The multiplicities of these two sites are 16 and 4, respectively [30, 31]. The NMR curve matches exactly this ratio, i.e., the sample has a perfect framework with high local orders.

The ^{29}Si MAS NMR of |ADA, F^-|-[SiO_2]-dodecasil 1H-**DOH** sample shows a good resolution of Q4 peaks, too. The hexagonal P/mmm (#191) unit cell has four unique T sites. Three corresponding Q4 peaks are resolved: δ = -115.12 ppm is the resonant of Si2/Si1; δ = -117.48 ppm belongs to Si1/Si3/Si4; δ = -120.76 ppm is attributed to Si3 [45].

|HMTA, F^-|-[SiO_2]-dodecasil 3C-**MTN** has three distinctive Si atoms in the cubic Fd3m (#227) unit cell, corresponding to the three well-resolved Q4 peaks in ^{29}Si MAS NMR at δ = -111.19, 115.52, and -118.87 ppm [46]. Unfortunately, there is an observable Q3 (-Si-(O-Si)$_3$) peak at δ = 101.65 ppm, indicating the existence of point defects in this particular material, which took an extremely long duration of 39 days for its crystallization at pH = 4. The peak area of the Q3 signal covers less than 5% of the total Si amount.

The ^{29}Si MAS NMR of |ADA, F^-|-[SiO_2]-deca-dodecasil 3R-**DDR** is less resolved in the Q4 region. Three Q4 peaks can be recognized, while the rhombohedral R-3m (#166) unit cell has seven unique T sites. Expected Q4 signals should populated in two groups, i.e., T6, T3 and T4

around -119 ppm, and T2, T1, T5 and T7 around -113 ppm [47]. The broaden peaks are resolvable in 2 or 3 bundles. In addition, there is a small Q3 peak observable at δ ~ 100 ppm, which is caused by point defects.

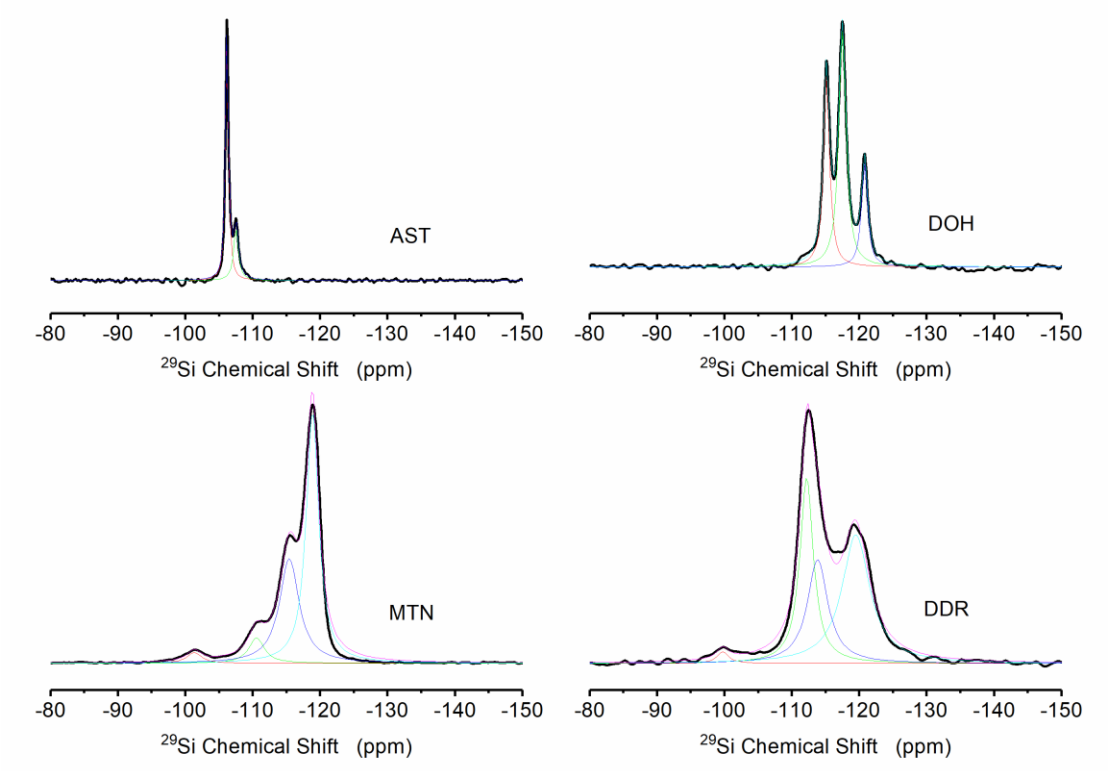

Figure 3. ^{29}Si MAS NMR of the acidic medium synthesized clathrasils.

3.3 The energetic aspects of |SDA, F^-|[SiO_2] compounds

As mentioned above, in the fluoride medium, especially under acidic conditions, the crystallization of clathrasils takes a relatively long time. The products are usually big crystals unless special methods are applied to reduce the crystal sizes.

It can be envisaged that the selection of a particular crystalline phase of the product in such slowly crystallizing systems would be less affected by kinetics parameters but overwhelmingly governed by energetic factors. Above all, the thermodynamic stability of the SDA@SiO_2 clathrasil intermediate would be the determining factor whether it crystallizes in the acidic system.

Here we illustrate a simple estimation of the thermodynamics of the SDA@SiO_2-framework systems by simulating the formation of the respective compounds of the dual components through energy minimization in a force field using the Monte Carlo method at 298 K and 101.3 kPa. At the current stage, a geometrical optimization of the frameworks, charging, and charge balancing of the SDA species in the acidic systems with F^- anions are temporarily not considered. The isosteric heats of SDA incorporation in the framework void spaces are taken as a measure of the energy release upon the compound formation. Two different simulated annealing programs (MS Sorption and MA Adsorption Locator) have been tested. The latter one includes molecular dynamic relaxations of the SDA and leads to higher isosteric heats.

Here we compare the values obtained from both methods in order to rank the thermodynamic stabilities of the SDA@Framework-SiO_2 compounds with the heat values (Table 3). Details of the SDA populations (Figure S1.1-S5.1) and the accompanied energy (Figure S1.2-S5.2) are illustrated in the Supplementary Information.

Table 3: The equilibrium loading of SDA at 298 K and 101.3 kPa in the void space of the frameworks and the simulated isosteric heats.

Framework	**SDA**	**Loading per unit cell**	**Loading per big cage**	**Isosteric heat** Sorption Locate (kcal/mol)	**Isosteric heat** Adsorption Locator (kcal/mol)
AST	TMA^+	4	$1/[4^6 6^{12}]$	10.545	17.400
DOH	ADA	1	$1/[5^{12} 6^8]$	26.429	44.240
MTN	HMTA	8	$1/[5^{12} 6^4]$	27.561	41.075
DDR	ADA	6	$1/[4^3 5^{12} 6^1 8^3]$	27.627	44.997
MFI	TPA^+	2	1/2 channel interactions	41.837	267.542

In the SDA@SiO_2-clathrasil systems, the full occupancies of the respective big cages with each SDA molecule/ion are readily established at 298 K and 101.3 kPa in the energy minimization procedure. Both simulated annealing methods suggest the same populated localizations of the SDAs around the geometrical centers of the big cages. Furthermore, the orientations of the SDAs, cannot be discriminated in the two methods. Figure 4 shows the locations of SDAs in the simulated framework cuts as the results of the simulated annealing.

Specifically, the TMA^+ cation takes the center of the $[4^6 6^{12}]$ cage of **AST**. The orientation is random due to the spherical shape of TMA^+. There are no specific short contacts between TMA^+ and the framework oxygens, because the sizes of the big cage and the relatively small TMA^+ cation do not match. The isosteric heat is low. The TMA^+ cation in this case, works merely as an unspecific space filler.

ADA molecule in **DOH** takes the center of the $[5^{12} 6^8]$ cage. The amino group points to the elongated direction of the cage down the [001] axis. None of the SDA atoms locates within a bonding distance to the framework oxygens.

ADA in **DDR** takes the center of the biggest cage, the $[4^3 5^{12} 6^1 8^3]$ 19-hedron, with full occupancy. The cage also possesses an ellipsoidal shape, but ADA inside has more freedom than in **DOH**. Thus, it can take a more random orientation.

HMTA is spherical, and it locates in the center of **MTN**'s $[5^{12} 6^4]$ cage with random orientations.

In comparison, TPA^+ in **MFI** occupies the channel intersection, with two opposite n-propyl chains stretching in the straight 10-ring channel and the two other n-propyl chains stretching into the sinusoidal channel. The terminal H atoms on the side chains should have stronger interactions with the O atoms of the channel walls. A half of the channel interactions is

occupied at 298 K and 101.3 kPa.

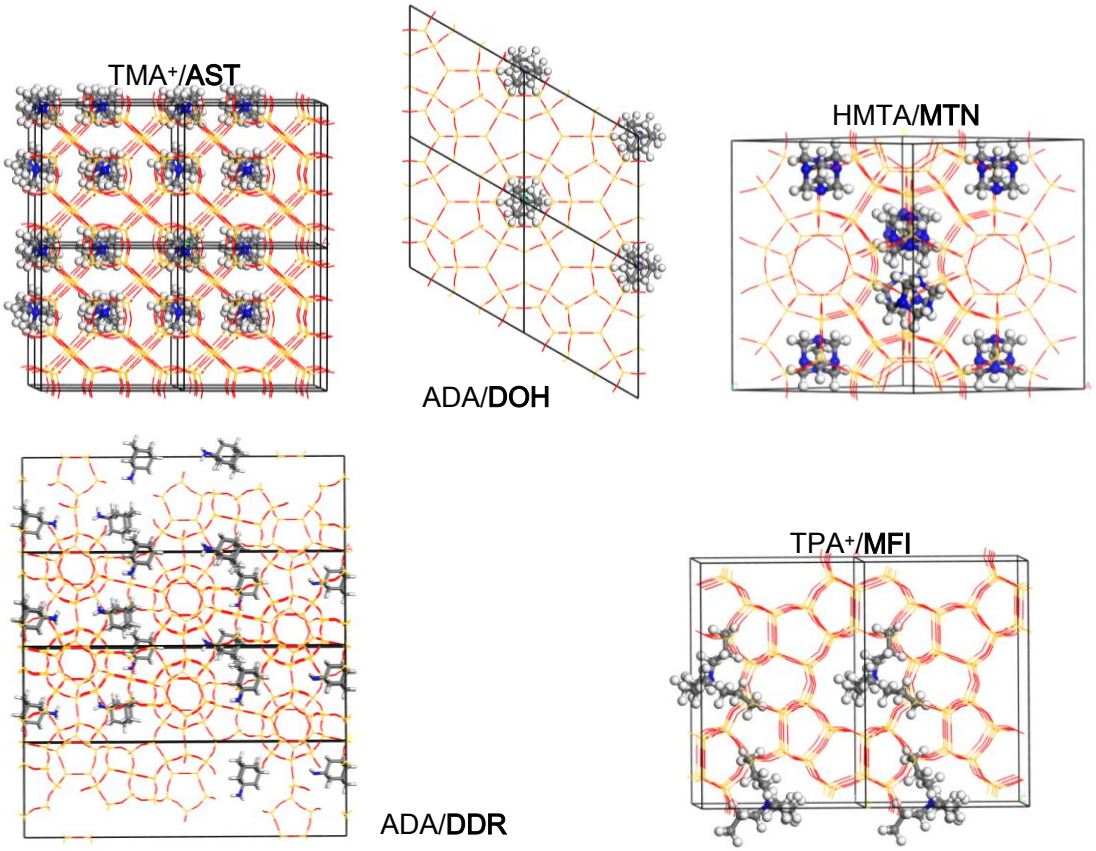

Figure 4. The occupancies and locations of respective SDA in the framework cuts, as found by simulated annealing: TMA^+/**AST**; ADA/**DOH**; HMTA/**MTN**; ADA/**DDR**; TPA^+/**MFI**.

The estimations of energetics are yet rough by ignoring the geometric relaxations of the frameworks and by not considering the charges and charge balances. However, it does give hints on the relative stabilities of the SDA@Framework-SiO_2 compounds. TPA^+/**MFI** has the highest isosteric heat and became the first material that has been synthesized in the acidic medium [25]. ADA/**DDR** releases more heat upon its formation than ADA/**DOH** does. Consequently, the former crystallizes at a lower temperature. The tested systems fall in the range of ca. 10 to 50 kcal/mol of isosteric heat. This kind of simulation test may be used in further dual systems of SDA@Framewrok-SiO_2 as an indicator to make quick predictions, whether the compound can be synthesized in an acidic medium.

3.4 The thermal decomposition and removal of the guests

TG/DTA of the acidic medium synthesized SDA@SiO_2 clathrasils show different thermal decomposition behaviors of the guest species under air (Figure 5). Table 4 reveals the differences between the theoretical guest weights at full occupancy and the total weight losses observed in the temperature ranges of room temperature to 1300^{o}C.

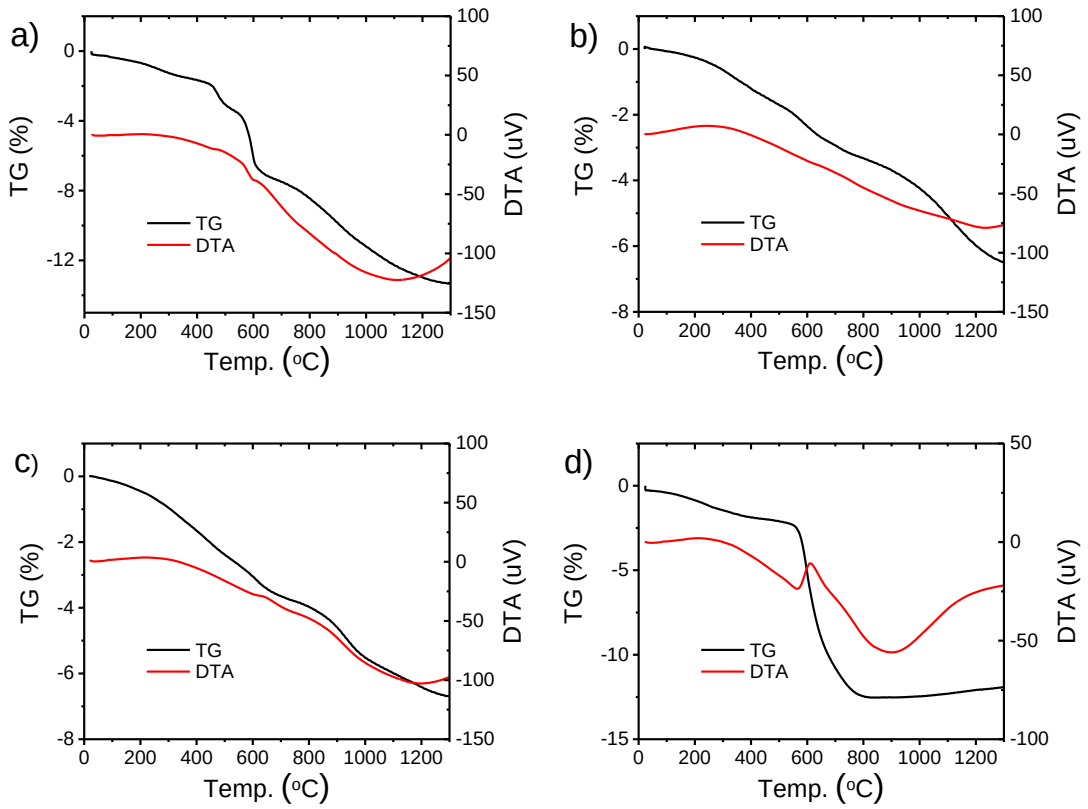

Figure 5. TG/DTA curves of the acidic medium synthesized SDA@SiO_2 clathrasils: a) TMA^+/**AST**; b) ADA/**DOH**; c) HMTA/**MTN**; and d) ADA/**DDR**.

The TG curve of TMA^+/**AST** displays a continuous, multi-stage weight loss. The first significant weight loss occurs at 470°C with -1.6 wt.%. The next one happens at 590°C, with -4.0 wt.%. Both events are accompanied by observable endothermic peaks in DTA. These are attributed to the decompositions of TMA^+, and migration of some decomposed pieces out of the big cage [31]. The manner that SDA leaves the clathrasil is sharply different from the one for zeolites, where exothermic combustion would usually occur at some lower temperatures, e.g., around 400°C. The small windows of clathrasil cages hindered the oxygen access which limits the SDA decomposition. Beyond these two peaks, the weight continues to decrease until the end of the experiment at 1300°C. A heat-flow in DTA that could be correlated with a structure collapse does not occur, i.e., the framework is extremely stable and stays intact at 1300°C. The theoretical TMA^+ content at the full occupancy approximates at 9.3 wt.%. The experimental total weight loss counts to 13.2 wt.%. The experimental value contains besides SDA decomposition also the desorption of adsorbed surface water (or water molecules occluded in the big cage with SDA), condensation of silanols, and leaching of F^- ions. Furthermore, even after the calcination at 1300°C, complete removal of the TMA^+ guest has not been achieved. The sample after the experiment has a black color, indicating that carbonous species are entrapped in the intra-crystalline voids. The TG/DTA process is very similar to the one of TMA^+/**AST** material crystallized in the near neutral medium reported by Villaescusa et al. [31].

Table 3: The calculated SDA weight contents at full occupancy in respective big cages, and the measured weight loss up to 1300°C under air.

	Theoretical SDA content* (wt.%)	TG weight loss upto 1300°C (wt.%)
TMA^+/AST	9.3	13.2
ADA/DOH	6.9	6.4
HMTA/MTN	12.1	6.6
ADA/DDR	11.2	12.1

* Possible F^- anions and adsorbed H_2O are not considered.

The decomposition of ADA and leaving from ADA/**DOH** material is almost continuous, with speeded stages recognizable at ca. 350, 600, and 1100°C, without significant heat events in DTA. The framework has survived the calcination at 1300°C, as well. The ADA removal is not completed, either. The experimental weight loss is 6.4 wt.%, vs. the theoretical guest loading of 6.9 wt.%.

In **MTN** framework, even the number of 6-ring windows of the biggest $[5^{12}6^4]$ cage is limited, consequently, a remarkable amount of carbonous species has been entrapped after the TG/DTA experiment, i.e., 6.6 wt.% weight loss vs. 12.1 wt.% HMTA content. Recognizable decomposition temperatures of HMTA are 590°C with a weak endothermic DTA peak, and 920°C, without a significant heat signal.

ADA can be completely removed from **DDR**, because it locates in the $[4^3 5^{12} 6^1 8^3]$ cage that has tree 8-ring windows. It starts to decompose at ca. 300°C, with the endothermic DTA peak at 565°C. Then, it ignites to combust, with a sharp weight loss completing at 800°C, accompanied by an exothermic DTA peak at 610°C. The weight loss from 500 to 800°C counts to 11.6 wt.%, matches the theoretical ADA content of 11.2 wt.%. The 1300°C calcined sample is white.

In general, the clathrasil compounds synthesized in an acidic medium possess extremely high framework stability. They all remain intact up to 1300°C in air. The decompositions of SDA species occur at higher temperatures than the combustion of SDA in zeolites. The removal of SDA out of the cages with maximum 6-ring windows cannot be completed by calcination at 1300°C. The ADA/**DDR** material is an exception, ADA can be combusted away completely at 610°C because the framework has 8-ring channels providing gas passages.

For comparison, the TG/DTA curves of the materials crystallized at higher pH are presented in Figure S6 in the Supplementary Information. In principle, they exhibit SDA cracking procedures very similar to their respective acidic medium counterparts. Minor differences are only seen at slightly more weight losses below ca. 200°C for desorption of surface water due to the smaller crystal sizes.

4. CONCLUSIONS

Protocols for the synthesis of clathrasil of the **AST**, **DOH**, **MTN,** and **DDR** topologies in

acidic medium (pH=2-6), using various amines and ammonium ions as SDAs, are elaborated.

The SDA species are encapsulated in the biggest cages of individual framework structures, with 1:1 full occupancy, around the geometric centers of the cages, as simulated annealing methods indicate.

The isosteric heats of the formation of these SDA@Framework-SiO_2 compounds are taken as a measure to evaluate the thermodynamic stabilities. And they are all lower than the TPA^+/**MFI** compound, which has been the first successful example of zeolite crystallization in an acidic medium. The rough values of the isosteric heats are in the range of 10 to 50 kcal/mol, obtained without considering geometrical optimizations of the frameworks and the charges and charge balances of the SDA@Framework-SiO_2 compound. This approach can be used to predict if an SDA@Framework-SiO_2 pair can crystallize in the acidic medium.

Last but not least, the success of the present syntheses points out that the method of zeolite crystallization in acidic medium is not only applicable to the synthesis of silicalite-1. It can be employed as a general method for the syntheses of porous tectosilicates of various framework topologies. New SDAs that do not work in the traditional basic and neutral systems can be found in the acidic chemistry. The zeolite synthesis in acidic medium is a broad chemistry field that remains almost unexplored so far. New framework structures and new chemical elements as framework buildingblocks are to be discovered. It opens ways leading to materials of new properties.

Supplementary Information

The populations and energy distributions of SDAs in the void spaces of respective frameworks, as energy minimization in pcff Force Field through Monte Carlo simulations, TG/DTA curves of materials synthesized at basic conditions, are available in Supplementary Information. The following files are available free of charge.

SupplementaryInformation.pdf

CRediT authorship contribution statement

H. Zhao: Investigation, Writing – original draft. **Q. Lang, G. Fu, R. Ding, S. Wang**: Investigation. **X. Yang**: Investigation, Methodology, Writing – original draft. **V. Valtchev**: Conceptualization, Supervision, Writing – review & editing, Funding acquisition.

Declaration of competing interest

The authors declare that they have no known competing financial interests or personal relationships that could have appeared to influence the work reported in this paper.

Acknowledgments

The ZeoMat Group acknowledges the starting grant provided by QIBEBT. V.V. and X.Y

acknowledge the collaboration in the framework of the Sino-French joint laboratory “Zeolites”.

REFERENCES

[1] J.L. Schlenker, F.G. Dwyer, E.E. Jenkins, W.J. Rohrbaugh, G.T. Kokotailo, W.M. Meier, Crystal structure of a synthetic high silica zeolite—ZSM-39, Nature, 294 (1981) 340-342.

[2] B. Kamb, A Clathrate Crystalline Form of Silica, Science, 148 (1965) 232-234.

[3] K. Momma, Clathrate compounds of silica, Journal of Physics: Condensed Matter, 26 (2014) 103203.

[4] F. Liebau, H. Gies, R.P. Gunawardane, B. Marler, Classification of tectosilicates and systematic nomenclature of clathrate type tectosilicates: a proposal, Zeolites, 6 (1986) 373 - 377.

[5] A.W.C.v.d. Berg, S. Bromley, E. Flikkema, J. Wojdel, T. Maschmeyer, J. Jansen, Molecular-dynamics analysis of the diffusion of molecular hydrogen in all-silica sodalite, The Journal of chemical physics, 120 21 (2004) 10285-10289.

[6] D. Bastani, N. Esmaeili, M. Asadollahi, Polymeric mixed matrix membranes containing zeolites as a filler for gas separation applications: A review, Journal of Industrial and Engineering Chemistry, 19 (2013) 375-393.

[7] M.J. den Exter, J.C. Jansen, H. van Bekkum, Separation of Permanent Gases on the All-Silica 8-Ring Clathrasil DD3R, in: J. Weitkamp, H.G. Karge, H. Pfeifer, W. Hölderich (Eds.) Studies in Surface Science and Catalysis, Elsevier1994, pp. 1159-1166.

[8] G. Kong, L. Fan, L. Zhao, Y. Feng, X. Cui, J. Pang, H. Guo, H. Sun, Z. Kang, D. Sun, S. Mintova, Spray-dispersion of ultra-small EMT zeolite crystals in thin-film composite membrane for high-permeability nanofiltration process, Journal of Membrane Science, 622 (2021)

119045.

[9] J.V. Smith, C.S. Blackwell, Nuclear magnetic resonance of silica polymorphs, Nature, 303 (1983) 223-225.

[10] K. Momma, T. Ikeda, K. Nishikubo, N. Takahashi, C. Honma, M. Takada, Y. Furukawa, T. Nagase, Y. Kudoh, New silica clathrate minerals that are isostructural with natural gas hydrates, Nature Communications, 2 (2011) 196.

[11] K. Momma, T. Ikeda, T. Nagase, T. Kuribayashi, C. Honma, K. Nishikubo, N. Takahashi, M. Takada, Y. Matsushita, R. Miyawaki, S. Matsubara, Bosoite, a new silica clathrate mineral from Chiba Prefecture, Japan, Mineralogical Magazine, 84 (2020) 941-948.

[12] H. Gies, F. Liebau, H. Gerke, “Dodecasils”–A Novel Series of Polytypic Clathrate Compounds of SiO2, Angewandte Chemie International Edition in English, 21 (1982) 206-207.

[13] H. Gerke, H. Gies, Studies on clathrasils. IV. Crystal structure of dodecasil 1 H, a synthetic clathrate compound of silica, Zeitschrift für Kristallographie - Crystalline Materials, 166 (1984) 11-22.

[14] H. Gies, 1-Aminoadamantane as guest molecule in dodecasil 1H: an X-ray crystallographic study, Journal of inclusion phenomena, 4 (1986) 85-91.

[15] H. Gies, Studies on Clathrasils. VI*, Zeitschrift für Kristallographie, 167 (1984) 73-82.

[16] H. Gies, Studies on clathrasils. IX*, Zeitschrift für Kristallographie - Crystalline Materials, 175 (1986) 93-102.

[17] B. Marler, N. Dehnbostel, H.H. Eulert, H. Gies, F. Liebau, Studies on clathrasils VIII. Nonasils-[4158], 88SiO2 · 8M8 · 8M9 · 4M20: Synthesis, thermal properties, and crystal structure, Journal of inclusion phenomena, 4 (1986) 339-349.

[18] K. Lu, Y. Fan, J. Huang, J. Wang, H. Xu, J. Jiang, Y. Ma, P. Wu, “Open” Nonporous Nonasil Zeolite Structure for Selective Catalysis, Journal of the American Chemical Society, (2021).

[19] L. McCusker, The ab initio structure determination of Sigma-2 (a new clathrasil phase) from synchrotron powder diffraction data, Journal of Applied Crystallography, 21 (1988) 305-310.

[20] A. Stewart, Synthesis and characterization of the novel tectosilicate sigma-2, Zeolites, 9 (1989) 140-145.

[21] A. Grünewald-Lüke, B. Marler, H. Gies, Crystal structure of clathrasil sigma-2 containing 3-azabicyclo[3.2.2]nonan as the guest molecule, ABN-sigma-2, (C8H15N)4[Si64O128], Zeitschrift für Kristallographie - New Crystal Structures, 216 (2001) 689-690.

[22] H. Gies, J. Rius, Ab-initio structure determination of zeolite RUB-10 from low resolution X-ray powder diffraction data, Zeitschrift für Kristallographie - Crystalline Materials, 210 (1995) 475-480.

[23] P. Caullet, J.L. Guth, J. Hazm, J.M. Lamblin, H. Gies, Synthesis, Characterization and Crystal-Structure of the New Clathrasil Phase Octadecasil, European Journal of Solid State and Inorganic Chemistry, 28 (1991) 345-361.

[24] D. Zhao, S. Qiu, W. Pang, Zeolites synthesized from nonalkaline media, in: R. von Ballmoos, J.B. Higgins, M.M.J. Treacy (Eds.) Proceedings from the Ninth International Zeolite Conference, Butterworth-Heinemann1993, pp. 337-344.

[25] D. Shi, K.-G. Haw, C. Kouvatas, L. Tang, Y. Zhang, Q. Fang, S. Qiu, V. Valtchev, Expanding the Synthesis Field of High-Silica Zeolites, Angewandte Chemie-International

Edition, 59 (2020) 19576-19581.

[26] X. Yang, E. Dib, Q. Lang, H. Guo, G. Fu, J. Wang, Q. Yi, H. Zhao, V. Valtchev, Silicalite-1 formation in acidic medium: Synthesis conditions and physicochemical properties, Microporous and Mesoporous Materials, 329 (2022) 111537.

[27] X. Yang, M.A. Camblor, Y. Lee, H. Liu, D.H. Olson, Synthesis and crystal structure of As-synthesized and calcined pure silica zeolite ITQ-12, J Am Chem Soc, 126 (2004) 10403-10409.

[28] A. Turrina, P.A. Cox, Molecular Modelling of Structure Direction Phenomena, in: L. Gómez-Hortigüela (Ed.) Insights into the Chemistry of Organic Structure-Directing Agents in the Synthesis of Zeolitic Materials, Springer International Publishing, Cham, 2018, pp. 75-102.

[29] C. Baerlocher, L.B. McCusker, D.H. Olson, Database of zeolite structures, www.iza-online.orgwww.iza-online.org.

[30] X.B. Yang, Synthesis and crystal structure of tetramethylammonium fluoride octadecasil, Materials Research Bulletin, 41 (2006) 54-66.

[31] L.A. Villaescusa, P.A. Barrett, M.A. Camblor, Calcination of Octadecasil: Fluoride Removal and Symmetry of the Pure SiO2 Host, Chemistry of Materials, 10 (1998) 3966-3973.

[32] D.M. Bibby, L.M. Parker, ZSM-39: Its preparation and some properties, Zeolites, 3 (1983) 11-12.

[33] Y. Long, H. He, P. Zheng, G. Wu, B. Wang, Single crystal growth, morphology, and structure of ZSM-39 and its variation CF-4, Journal of inclusion phenomena, 5 (1987) 355-362.

[34] P. Wagner, Y. Nakagawa, G.S. Lee, M.E. Davis, S. Elomari, R.C. Medrud, S.I. Zones, Guest/Host Relationships in the Synthesis of the Novel Cage-Based Zeolites SSZ-35, SSZ-36,

and SSZ-39, Journal of the American Chemical Society, 122 (2000) 263-273.

[35] M.A. Camblor, L.A. Villaescusa, M.J. Díaz-Cabañas, Synthesis of all-silica and high-silica molecular sieves in fluoride media, Topics in Catalysis, 9 (1999) 59-76.

[36] S.I. Zones, A.W. Burton, G.S. Lee, M.M. Olmstead, A Study of Piperidinium Structure-Directing Agents in the Synthesis of Silica Molecular Sieves under Fluoride-Based Conditions, Journal of the American Chemical Society, 129 (2007) 9066-9079.

[37] D. Schwalbe-Koda, S. Kwon, C. Paris, E. Bello-Jurado, Z. Jensen, E. Olivetti, T. Willhammar, A. Corma, Y. Román-Leshkov, M. Moliner, R. Gómez-Bombarelli, A priori control of zeolite phase competition and intergrowth with high-throughput simulations, Science, 374 (2021) 308-315.

[38] R.F. Lobo, S.I. Zones, M.E. Davis, Structure-direction in zeolite synthesis, Journal of inclusion phenomena and molecular recognition in chemistry, 21 (1995) 47-78.

[39] Y. Kubota, M.M. Helmkamp, S.I. Zones, M.E. Davis, Properties of organic cations that lead to the structure-direction of high-silica molecular sieves, Microporous Materials, 6 (1996) 213-229.

[40] L. Gómez-Hortigüela, M.Á. Camblor, Introduction to the Zeolite Structure-Directing Phenomenon by Organic Species: General Aspects, in: L. Gómez-Hortigüela (Ed.) Insights into the Chemistry of Organic Structure-Directing Agents in the Synthesis of Zeolitic Materials, Springer International Publishing, Cham, 2018, pp. 1-41.

[41] E.W. Valyocsik, Crystalline silicate ZSM-58 and process for its preparation using a methyltropinium cation, U.S. Patent 4,698,217A, (1987).

[42] J. Weitkamp, S. Ernst, T. Bock, A. Kiss, P. Kleinschmit, Introduction of noble metals into

small pore zeolites via solid state ion exchange, in: H.K. Beyer, H.G. Karge, I. Kiricsi, J.B. Nagy (Eds.) Studies in Surface Science and Catalysis, Elsevier1995, pp. 278-285.

[43] E. Hayakawa, S. Himeno, Synthesis of all-silica ZSM-58 zeolite membranes for separation of CO2/CH4 and CO2/N2 gas mixtures, Microporous and Mesoporous Materials, 291 (2020) 109695.

[44] P. Caullet, J.-L. Paillaud, A. Simon-Masseron, M. Soulard, J. Patarin, The fluoride route: a strategy to crystalline porous materials, Comptes Rendus Chimie, 8 (2005) 245-266.

[45] E.J.J. Groenen, N.C.M. Alma, J. Dorrepaal, G.R. Hays, A.G.T.G. Kortbeek, Solid-state 29Si n.m.r. spectroscopy of clathrasils; the relationship between the chemical shift and the structure of silicates, Zeolites, 5 (1985) 361-363.

[46] H. Strobl, C.A. Fyfe, G.T. Kokotailo, C.T. Pasztor, D.M. Bibby, High-symmetry, high-temperature zeolite lattice structures, Journal of the American Chemical Society, 109 (1987) 4733-4734.

[47] C.A. Fyfe, H. Gies, Y. Feng, H. Grondey, Two-dimensional 29Si MAS n.m.r. investigation of the three-dimensional structure of zeolite DD3R, Zeolites, 10 (1990) 278-282.